Current Status of LUMIO Mission

Characterizing Lunar Meteoroid Impacts with a CubeSat

Topputo, Francesco; Merisio, G.; Giordano, G.; Franzese, V; Cervone, A.; Speretta, S.; Menicucci, A.; Bertels, E.; Thorvaldsen, a.; More Authors

Publication date
2021

Document Version
Final published version

Citation (APA)
Topputo, F., Merisio, G., Giordano, G., Franzese, V., Cervone, A., Speretta, S., Menicucci, A., Bertels, E., Thorvaldsen, A., & More Authors (2021). *Current Status of LUMIO Mission: Characterizing Lunar Meteoroid Impacts with a CubeSat*. Paper presented at 72nd International Astronautical Conference, Dubai, United Arab Emirates.

72nd International Astronautical Congress (IAC), Dubai, United Arab Emirates, 25-29 October 2021.

IAC-21,A3,2A,5,x65923

Current Status of LUMIO Mission: Characterizing Lunar Meteoroid Impacts with a CubeSat

Francesco Topputo[1], Gianmario Merisio[2], Carmine Giordano[3], Vittorio Franzese[4], Mauro Massari[5], Pierluigi Di Lizia[6], Demetrio Labate[7], Giuseppe Pilato[8], Angelo Cervone[9], Stefano Speretta[10], Alessandra Menicucci[11], Eric Bertels[12], Andreas Thorvaldsen[13], Andrei Kukharenka[14], Johan Vennekens[15], Roger Walker[16]

The Lunar Meteoroid Impact Observer (LUMIO) is a mission designed to observe, quantify, and characterize the impacts of meteoroids on the lunar far side and, therefore, complement in both space and time the observations currently taken from Earth. While Earth-based lunar observations are restricted by weather, geometric and illumination conditions, a Moon-based observation campaign can improve the detection rate of impact flashes and the general quality and reliability of the final scientific product. The mission has successfully completed the Phase A design, after successfully passing Phase 0 and an independent study in the ESA Concurrent Design Facility that has fully confirmed its feasibility. The LUMIO spacecraft is a 12U XL CubeSat with a mass of around 28 kg, released into Lunar orbit by a carrier spacecraft and capable of autonomously transferring from this initial parking orbit to its final destination, a halo orbit about the Earth–Moon L_2 point from which permanent full-disk observation of the Lunar far side can be performed. The mission objectives will be achieved thanks to the LUMIO-Cam, a custom-designed optical instrument capable of detecting light flashes in the visible spectrum, and an innovative on-board data processing system, capable of drastically reducing the amount of information that needs to be transmitted back to Earth. The camera is capable of generating $5\,\mathrm{TB\,d^{-1}}$ of data, out of which only approximately $1\,\mathrm{MB\,d^{-1}}$ will need to be transmitted to Earth, since impact identification will be performed autonomously onboard and only relevant information will be actually transmitted. This paper will present the current status of the mission, summarising the main results of the Phase A design and the way forward to the following steps in mission implementation (Phases B-C). The paper will include a summary of the spacecraft system design and mission analysis. Particular focus will be given to the mission operations aspects.

1 Introduction

The Earth–Moon system is constantly bombarded by meteoroids of different sizes, and their numbers are significant. Fragments of asteroids and comets, that date back to planetary formation times, constantly encounter the Earth and Moon in their orbits, and impact them as meteoroids. Observations of meteor showers on Earth have been studied for at least 50 years [1], in order to construct Solar System meteoroid models. These models can be useful in, e. g., predicting the small-meteoroid flux that deteriorates space equipment or when the next

[1]Full Professor, Department of Aerospace Science and Technology, Politecnico di Milano, Via La Masa 34, 20156, Milano, Italy; francesco.topputo@polimi.it
[2]PhD Student, Department of Aerospace Science and Technology, Politecnico di Milano, Via La Masa 34, 20156, Milano, Italy, gianmario.merisio@polimi.it
[3]PostDoc Researcher, Department of Aerospace Science and Technology, Politecnico di Milano, Via La Masa 34, 20156, Milano, Italy, carmine.giordano@polimi.it
[4]PostDoc Researcher, Department of Aerospace Science and Technology, Politecnico di Milano, Via La Masa 34, 20156, Milano, Italy, vittorio.franzese@polimi.it
[5]Associate Professor, Department of Aerospace Science and Technology, Politecnico di Milano, Via La Masa 34, 20156, Milano, Italy, mauro.massari@polimi.it
[6]Assistant Professor, Department of Aerospace Science and Technology, Politecnico di Milano, Via La Masa 34, 20156, Milano, Italy, pierluigi.dilizia@polimi.it
[7]Program Manager, Leonardo S.p.A., Via delle Officine Galileo 1, 50013, Campi Bisenzio, Firenze, Italy, demetrio.labate@leonardocompany.com
[8]Engineer, Leonardo S.p.A., Via delle Officine Galileo 1, 50013, Campi Bisenzio, Firenze, Italy, giuseppe.pilato@leonardocompany.com
[9]Assistant Professor, TU Delft, Kluyverweg 1, 2629 HS, Delft, The Netherlands, a.cervone@tudelft.nl
[10]Assistant Professor, TU Delft, Kluyverweg 1, 2629 HS, Delft, The Netherlands, s.speretta@tudelft.nl
[11]Assistant Professor, TU Delft, Kluyverweg 1, 2629 HS, Delft, The Netherlands, a.menicucci@tudelft.nl
[12]Systems Engineer, ISIS-Innovative Solutions in Space, Motorenweg 23, 2623 CR, Delft, The Netherlands, e.bertels@isispace.nl
[13]SW Engineer, Science and Technology AS, Tordenskiolds Gate 6, 0160, Oslo, Norway, thorvaldsen@stcorp.no
[14]SW Engineer, Science and Technology AS, Tordenskiolds Gate 6, 0160, Oslo, Norway, kukharenka@stcorp.no
[15]Systems Engineer, European Space Research & Technology Centre (ESTEC), ESA, Keplerlaan 1, 2201 AZ, Noordwijk, The Netherlands, johan.vennekens@esa.int
[16]Head of CubeSat Systems Unit, European Space Research & Technology Centre (ESTEC), ESA, Keplerlaan 1, 2201 AZ, Noordwijk, The Netherlands, roger.walker@esa.int

large meteoroid will impact the Earth itself. As meteoroids originate from asteroids and comets, meteoroid models can also be used to understand the spatial distribution of those objects near the Earth–Moon system.

By observing the lunar surface impacts, whose flux is similar to that of the Earth, we could obtain detailed information regarding their magnitudes, velocities, temporal and spatial distributions. These information can be used to increase confidence of meteoroid models, to validate the existing lunar impact models, to contribute to lunar seismology studies and interior modeling, and to initiate a Lunar Situational Awareness programme for future exploration missions.

Earth-based optical observations of the light flashes produced by lunar meteoroid impacts have revealed useful in the validation and improvement of meteoroid models [2]. Monitoring the Moon for meteoroid impact flashes allows for the observation of larger areas than those covered by traditional surveys of Earth's upper atmosphere. Thus, theoretically, more meteoroid impacts can be detected in shorter periods of time [3]. Moreover, Earth-based lunar observations are restricted by weather, geometric, and illumination conditions. As such, a lunar CubeSat can improve the detection rate of lunar meteoroid impact flashes, as it would allow for longer monitoring periods. Moreover, it being closer to the Moon surface, a lunar CubeSat could also allow for the detection of meteoroids smaller than millimeters [4].

In this work, the current status of the mission is presented. The main results of the Phase A design and the way forward to the following steps in mission implementation (Phases B-C) are discussed too. The paper will include a summary of the spacecraft system design and mission analysis. Particular focus will be given to the mission operations aspects.

The remainder of the paper is organized as follows. In Section 2 an overview of the mission is provided. The description of the payload modeling follows in Section 3. The most recent results about the radiometric analysis and the estimated payload data return are presented in Section 4 and Section 5, respectively. Concluding remarks are given in Section 6.

2 Mission overview

LUMIO is a CubeSat mission to a halo orbit at Earth–Moon L_2 that shall observe, quantify, and characterize meteoroid impacts on the Lunar farside by detecting their flashes, complementing Earth-based observations on the Lunar nearside, to provide global information on the lunar meteoroid environment and contribute to lunar situational awareness.

LUMIO was awarded ex-aequo winner of the European Space Agency's challenge LUCE, under the SysNova framework, and as such it is being considered for implementation in the near future. The Phase A study has been conducted in 2020 and successfully completed at the beginning of 2021 under ESA's General Support Technology Programme (GSTP) contract. It has received support from the national delegations of Italy (ASI), the Netherlands (NSO), and Norway (NOSA). That after a successful, independent mission assessment performed by ESA's Concurrent Design Facility (CDF) team. The consortium of the Phase A study is formed by Politecnico di Milano, Leonardo S.p.A., ISISPACE, Delft University of Technology, and S[&]T Norway.

LUMIO mission is conceived to address the following issues:

- **Science question**. What are the spatial and temporal characteristics of meteoroids impacting the lunar surface?
- **Science goal**. Advance the understanding of how meteoroids evolve in the cislunar space by observing the flashes produced by their impacts with the lunar surface.
- **Science objective**. Characterize the flux of meteoroids impacting the lunar surface.

LUMIO wants to quantify the luminous energy of meteoroid impacts to the Moon in the equivalent kinetic energy range at the Earth from 10^{-6} to 10^{-4} kton TNT. That because observations reported in literature have significant error margins and also a set of discrepancies is observed [5, 6]. Additionally, the mission aims to detect new meteoroid impacts to the Moon in the kinetic energy range from 10^{-4} to 10^{-1} kton TNT. Indeed, no events have ever been recorded in the latter range [5, 6].

The list of top-level objectives of LUMIO is shown in Tab. 1. Then, the list of the mission objectives follows in Tab. 2. Finally, the technology demonstration (also referred to as tech-demo) objectives are presented in Tab. 3.

The mission utilizes a 12U XL form-factor CubeSat which carries the LUMIO-Cam, an optical instrument capable of detecting light flashes in the visible spectrum to continuously monitor and process the data. The mission implements a novel orbit design [7] and commercial-off-the-shelf (COTS) CubeSat technologies, to serve as a pioneer in demonstrating how CubeSats can become a viable tool for interplanetary science and exploration.

The mission is made up of five different phases. Namely:

1. **Launch**. The LUMIO spacecraft is designed to be launched as part of one of the CLPS missions (baseline launch option) or as piggyback payload of Artemis 2 mission (backup launch option).

Tab. 1: Top-level objectives.

Objective ID	Objective	Stakeholder
TLO.01	To perform remote sensing of the lunar surface and measurement of astronomical observations not achievable by past, current, or planned lunar missions.	ESA
TLO.02	To demonstrate deployment and autonomous operation of CubeSats in lunar environment, including localization and navigation aspects.	ESA
TLO.03	To demonstrate miniaturization of optical instrumentation and associate technology in lunar environment.	ESA
TLO.04	To perform inter-satellite link to a larger Lunar Orbiter for relay of data and for TT&C.	ESA

Tab. 2: Mission objectives.

Objective ID	Objective	Stakeholder
MO.01	To conduct observations of the lunar surface in order to detect meteoroid impacts and characterize their flux, magnitudes, luminous energies, and sizes.	ESA
MO.02	To complement observations achievable via ground-based assets in space, time, and quality in order to provide a better understanding of the meteoroid environment.	ESA

Tab. 3: Tech-demo objectives.

Objective ID	Objective	Stakeholder
TDO.01	To perform autonomous navigation experiments by using images of the Moon.	ESA, Polimi
TDO.02	To demonstrate CubeSat trajectory control capabilities into lunar environment.	Polimi
TDO.03	To demonstrate the use of miniaturized optical payload in lunar environment.	Leonardo S.p.A.
TDO.04	To demonstrate the use of miniaturized technologies into lunar environment.	ISISPACE
TDO.05	To demonstrate the use of miniaturized propulsion systems in lunar environment.	TU Delft
TDO.06	To perform autonomous, high-performance onboard payload data processing.	S[&]T

2. **Earth–Moon transfer phase**. LUMIO is carried inside its mothership to the Lunar parking orbit. During the transfer the spacecraft is switched off inside its deployer and a power connection with the mothership keeps the batteries charged.
3. **Parking phase**. The CubeSat is released in its Lunar parking orbit (expected to be highly elliptical) by the mothership. After de-tumbling and deployment of the solar arrays, the payload and all subsystems are commissioned. The spacecraft cruises with radiometric navigation strategy and direct-to-Earth (DTE) communication and performs, when necessary, station keeping and wheel desaturation maneuvers.
4. **Transfer phase**. LUMIO transfers from the parking orbit to its final operative orbit. A total of four maneuvers are executed during the transfer: a stable manifold injection maneuver, two trajectory correction maneuvers, and a halo injection maneuver. The spacecraft cruises with radiometric navigation strategy and DTE communication and performs, when necessary, wheel desaturation maneuvers.
5. **Operative phase**. During this phase the spacecraft accomplishes its scientific objectives. The nominal duration of the phase is 1 year, and it is subdivided in two periodical cycles: *i*) the *science cycle*, during which the scientific data are continuously acquired, processed on board and compressed, and *ii*) the *navigation & engineering* cycle, during which radiometric navigation based on DTE link is performed (in parallel with the demonstration of an autonomous optical navigation experiment using the LUMIO-Cam [8]), and station keeping and wheel desaturation maneuvers are conducted. With reference to Fig. 1, the science cycle takes place during the portion of the lunar cycle when the illumination of the Moon allows for scientific observations (solid blue line), while the navigation & engineering cycle will take place when scientific observations of the lunar farside are not possible (solid orange line).
6. **End-of-life phase**. In this phase, all spacecraft systems are de-commissioned, and the end of life maneuver is performed.

A quasi-periodic halo orbit about Earth–Moon L_2 is the designated operative orbit for LUMIO. The selection of the operative orbit is the result of a thorough trade-off analysis performed during the Phase 0 study [7]. According to the assumed timeline of the mission, the operative phase is expected to start on 21 March 2024, and to end on 22 March 2025. Different views of the nominal quasi-halo orbit are shown in Fig. 2. The trajectory is represented in the Earth–Moon roto-pulsating frame in dimensionless coordinates. The ranges of LUMIO from the Moon and the Earth are plotted in Fig. 3. On average, the range from the Moon is 60 000 km, while that from the Earth is 444 000 km.

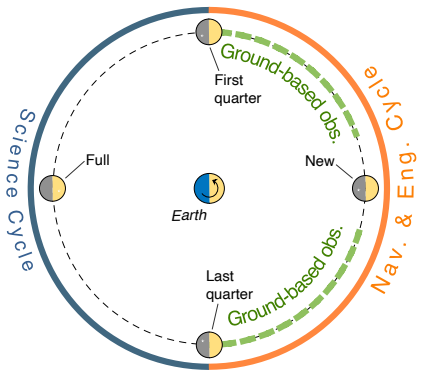

Fig. 1: Science and navigation & engineering cycles in relation to Moon phases.

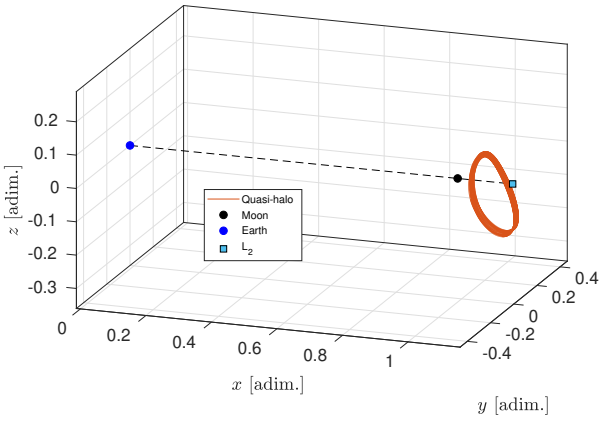

Fig. 2: Different views of selected operative Earth–Moon L_2 quasi-halo orbit in the Earth–Moon roto-pulsating frame in dimensionless coordinates.

2.1 *LUMIO-Cam payload*

The LUMIO-Cam is a custom payload developed by a key partner of LUMIO consortium. The LUMIO-Cam implements two channel, each equipped with a CCD having 1024x1024 active pixels, associated to an optics with a field of view of 6 deg and 127 mm focal length. The sensitivity of the chosen detector extends from visible to near-infrared spectrum, thus allowing for a wide range of exploitation of the impact radiation emissions. After the optics, a dichroic beam splitter divides the incoming signal in two channels. One receiving the signal in the visible spectrum and the other in the near-infrared.

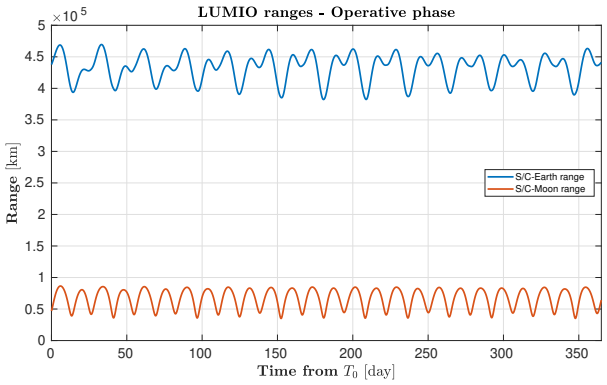

Fig. 3: LUMIO's ranges from the Moon and the Earth during the operative phase.

Finally, the signal is detected by the two CCD. The resulting mass including margins at the current stage of the design is 2.88 kg. The estimated maximum power consumption including margins is 18.8 W. A rendering of the current camera design is shown in Fig. 4.

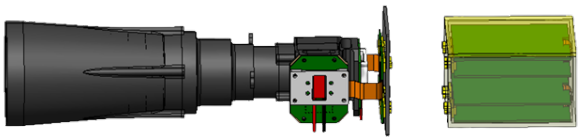

Fig. 4: LUMIO-Cam overall architecture. From left to right: optical head, focal plane assembly, and proximity electronic.

2.2 Overview of the platform

The Phase A study of the LUMIO CubeSat is the third iteration of the design. The first iteration was represented by the design proposed in response to the SysNova LUCE challenge, while the second iteration was obtained by including modifications suggested by ESA's CDF team. Fig. 5 shows the current LUMIO CubeSat exterior configuration. LUMIO is designed to survive for 1.5 years in space. At the present day, the mass of the CubeSat including margins is estimated to be 28.66 kg. The Cubesat, is capable of producing between 53.5 and 58.0 W, and storing up to 90 W h in the equipped lithium-ion batteries. It can communicate both in S- and X-band. The propulsion system, which is based on a pressurized monopropellant, is designed to provide a total ΔV of 220 m s^{-1}. The most important figures and performances of the LUMIO satellite platform are listed in Tab. 4.

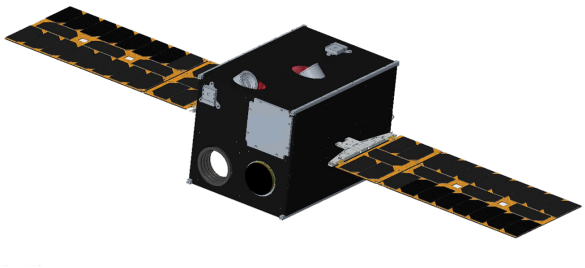

Fig. 5: LUMIO lunar CubeSat configuration.

3 Modelling of the LUMIO-Cam

The peculiarity of the LUMIO-Cam is the presence of two channels, the visible spectrum channel (VIS) and the near-infrared wavelength range channel (NIR). The incoming light is split at 820 nm by means of a dichroic. Each channel is equipped with the same CCD detector. The LUMIO-Cam takes pictures with exposure time Δt_{exp} = 66 ms, meaning that the payload works at 15 fps. The list of LUMIO-Cam specifics is presented in Tab. 5. Currently, an entrance baffle 150 mm grants that no direct sunlight hits first lens at sun angles larger than 20 deg [9].

The signal-to-noise ratio (SNR) is defined in [10] as

$$\mathrm{SNR} = \frac{s_i}{\sigma} \tag{1}$$

where s_i is the signal, in e$^-$, of a generic source of interest while σ is the Poisson noise, in e$^-$ *rms* (Root-Mean-Square), associated with all signals collected by the detector. The signal s_i and σ refer to the single pixel. The Poisson noise of a source i is given by [10]

$$\sigma_i = \sqrt{s_i} \tag{2}$$

while the total Poisson noise is obtained as follows [10]

$$\sigma = \sqrt{\sum_i \sigma_i^2} = \sqrt{\sum_i s_i}. \tag{3}$$

In the specific case of the LUMIO-Cam, the Signal-to-Noise Ratio (SNR) of an impact flash must be computed for both VIS and NIR.

3.1 Impact flash duration in LUMIO-Cam frames

It is assumed that the channels are perfectly synchronized, therefore, they take pictures of the Moon simultaneously. Generally speaking, a flash may occur at any time, which means that the starting times of the impact flash and the photographic frame may not coincide. The flash duration in simultaneous frames of the two channels is exactly the same. This assumption is not true in

Tab. 4: CubeSat performances and characteristics.

Property	**Value/Specific**	**Remarks**
Platform		
Size	12U XL	ISISPACE deep-space deployer compatible
Mass	28.66 kg	-
Design lifetime	1.5 years	-
Electrical power system		
Power generation	53.5-58.0 W	Worst case scenario
Power storage	90 W h	Lithium-ion batteries
Payload power	Up to 18.8 W	-
Break out voltages	14.5-16.0 V	Unregulated battery voltage
Command & data handling		
Data bus protocol	CAN	-
Operating system	FreeRTOS	-
On-board storage	64 GB	-
Communication (TT&C and payload)		
Frequency	S-band	Inter-satellite link
	X-band	Direct-to-Earth
Propulsion system		
Type	Pressurized monopropellant	Liquid propellant
Total ΔV	220 m s^{-1}	-

Tab. 5: LUMIO-Cam specifics.

Specific	**Symbol**	**Value**
CCD detector	ID	e2v CCD201-20
Focal length	FL	127 mm
F number	$F_{\#}$	2.5
Aperture diameter	D	50.80 mm
Field of view	FOV	6 deg
Sensitivity range	$[\lambda_1, \lambda_2]$	$[450, 950]$nm
Dichroic wavelength	λ_{dic}	820 nm
Active pixels	N_{pix}	1 Mpixel
Pixel size	d_{pix}	13.3 µm
Exposure time	Δt_{exp}	66 ms
Frame per second	FPS	15 fps
Low noise gain	G	$[1, 1000]$
Excess noise factor	F	$\sqrt{2}$
Polychromatic ensquared energy in 1 pixel	f_{ensq}	0.89
Dichroic transmissivity	η_{dic}	0.9

the real world, but it is assumed that the synchronization errors are negligible with respect to the integration time of a frame.

3.2 Signal peak location

In this study, it is assumed that the impact occurs close to the sub-satellite point and that the signal peak is contained in the central pixel of the LUMIO-Cam CCD detector. Specifically, 3 significant cases are identified:

1. the peak location is exactly at the centre of the pixel and the impact flash is completely contained within 1 pixel (spread fraction equal to 1);
2. half of the point spread function of the impact flash is contained within the pixel, which is expected to be the most common case (spread fraction equal to 1/2);
3. the peak location coincides with one of the 4 corners of the pixel (spread fraction is equal to 1/4).

3.3 Impact flash signal

The procedure to compute the signal coming from the impact flash is based on the fact that the impact raises a plume made of ejecta material. Such plume emits radiation which can be detected. An equivalent black body temperature is associated to the radiating plume. Generally speaking, the radiating plume cools down after the impact, hence, the equivalent black body temperature decreases in time [11]. The cooling process is not modeled in MeGun. Nevertheless, MeGun computes an equivalent black body temperature assumed constant in time.

To compute the signal, it has been taken into account: the sensitive spectrum range of the LUMIO-Cam, the dichroic wavelength, the aperture diameter, the frac-

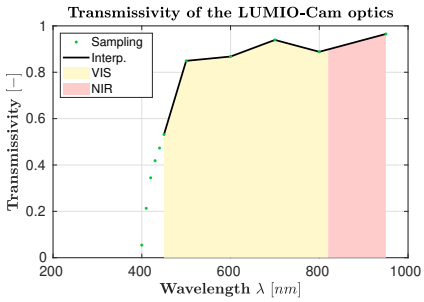

Fig. 6: Transmissivity of the LUMIO-Cam optics, dichroic contribution not included. The bandwidths received by VIS and NIR channels are highlighted with different colours. Sampling points are represented by point markers. The curve is a piecewise linear interpolation performed with MATLAB®.

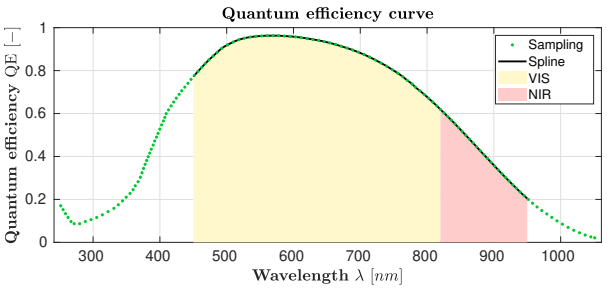

Fig. 7: QE curve of CCD201-20 detector. The bandwidths received by VIS and NIR channels are highlighted with different colours. Sampling points are represented by point markers. The curve is a spline interpolation performed with MATLAB®.

tion of polychromatic ensquared energy in 1 pixel, the attenuation effects of the optics (bulk absorption, real coating transmission, dichroic lens transmission), the quantum efficiency (QE) of the equipped CCD detector, the gain of the LUMIO-Cam, the distance from the impact location, and the impact dynamics (equivalent black body temperature of the plume, plume area, and flash duration).

Attenuation effects of the optics. The presence of optics causes some attenuation effects acting on the signal. The transmissivity defines the number of photons which do not get reflected by the optics. The curve describing the transmissivity of the optics at the wavelengths corresponding to the sensitive spectrum range of the camera is shown in Fig. 6. The curve takes into account how the bulk absorption and the real coating affect the transmissivity $\xi(\lambda)$ of the LUMIO-Cam. Regarding how the dichroic lens affects the performance of the LUMIO-Cam, it is assumed that the dichroic transmissivity is equal to $\eta_{\text{dic}} = 0.9$.

Quantum Efficiency of the CCD detector. The QE is used to convert the photons number at a given wavelength into a number of electrons. The QE curve of the selected detector is shown in Fig. 7.

Distance from the impact location. For the radiometric analysis, the minimum, the average, and the maximum distances of the LUMIO CubeSat from the centre of the Moon during the operative phase of the mission have been used as case studies. Specifically, they are: $r_{\text{min}} = 35\,878\,\text{km}$, $r_{\text{mean}} = 61\,048\,\text{km}$, and $r_{\text{max}} = 86\,218\,\text{km}$. The distance from the impact location is computed subtracting the radius of the Moon to the LUMIO–Moon distance.

Impact dynamics. To perform the radiometric analysis, the impact dynamics quantities needed to compute the SNR are retrieved simulating the meteoroid environment with MeGun [12].

3.4 Computation of the flash signal

The formula of the impact flash signal s_{imp} is [12]

$$\begin{aligned} s_{\text{imp}} &= \frac{A_{\text{oa},\perp}}{A_d} A_p \tau_i \int_{\lambda_1}^{\lambda_2} N_{e^-}(\lambda, T_{\text{imp}}) \text{d}\lambda \\ &= \frac{D^2 \cos(\theta)}{4\ f d_{\text{imp}}^2} A_p \tau_i \int_{\lambda_1}^{\lambda_2} N_{e^-}(\lambda, T_{\text{imp}}) \text{d}\lambda \end{aligned} \tag{4}$$

where $A_{\text{oa},\perp} = \pi D^2 \cos(\theta)/4$ is the surface of optics aperture perpendicular to the vector pointing towards the impact location, $A_d = f\pi d_{\text{imp}}^2$ is the area used to scale the signal at observer distance, D is the aperture diameter, θ is the angle between the boresight direction and the vector pointing towards the impact location, which is zero, since it is assumed that the impact happens at the sub-satellite point, f is the anisotropy degree used in MeGun, τ_i is the flash duration in the frame considered, A_p is the radiating plume area, $[\lambda_1, \lambda_2]$ is the domain in which the function $N_{e^-}(\lambda, T)$ is integrated. Note that, due to the presence of the dichroic, the integration domains for VIS and NIR are different.

3.5 Noise sources

The noise sources taken into account in the SNR computation are:

- the noise associated with the impact signal itself σ_{imp} (or photon shot noise);
- the straylight noise due to roughness, contamination, and ghosts σ_{sl};
- the moon surface background noise $\sigma_{\text{☾}}$;

- the dark current (or internal noise of CCD) σ_{DC};
- the readout noise of CCD σ_{RON};
- the off-chip noise of CCD σ_{OCN};
- the quantization noise generated by the analogue to digital converter σ_{QN}.

The detectors mounted in the two channels allow to amplify the signals generated in the pixels before the multiplication register by a factor G. Such signals are: s_{imp}, s_{sl}, $s_{\mathbb{C}}$, and s_{DC}. The gain G may be varied from $1\times$ to $1000\times$. The signal amplification increases also the total Poisson noise. That is accounted by means of the excess noise factor F. The expression to evaluate the SNR is

$$\mathrm{SNR} = 10\log_{10}\Big(Gs_{\mathrm{imp}}\big(F^2\ G\big(\sigma^2_{\mathrm{imp}}+\sigma^2_{\mathrm{sl}}+\sigma^2_{\mathbb{C}}+ \\ +\sigma^2_{\mathrm{DC}}\big)+\sigma^2_{\mathrm{RON}}+\sigma^2_{\mathrm{OCN}}+\sigma^2_{\mathrm{QN}}\big)^{-\frac{1}{2}}\Big) \tag{5}$$

where the results is in dB. If the signal is not amplified ($G = 1$) the excess noise factor should not be included in the formula. The numerical value taken from the detector's datasheet and used for the excess noise factor is $F = \sqrt{2}$.

4 Radiometric analysis results

To be conservative, the radiometric analysis has been performed setting the minimum SNR to 10 dB. Since the results have been obtained relying on the statistical approach of MeGun, the condition of saturation is not clearly demarcated. Therefore, the saturation condition has been set to occur when more than half of the impacts at specific conditions saturate the detector.

The firs set of results is about how the SNR varies with respect to the the impact kinetic energy of the meteoroid expressed in Earth equivalents. Results are shown in Fig. 8. The charts present the different behavior of the two channels at different distances of LUMIO from the Moon and for the 3 significant case studies of signal peak location. The impact energies that saturate the detector are highlighted in yellow. The charts have been plotted fixing the gain of the LUMIO-Cam at 10. For each given impact kinetic energy, 1000 impacts have been simulated to obtain the average SNR.

Clearly the range of impact kinetic energies which can be detected depend strongly on the distance from the Moon and on the spread fraction of the impact flash on the pixel. The most common case should be the one in which the spread fraction is 1/2. From the chart, it is clear that keeping the gain fixed does not allow to cover properly the whole range of impact kinetic energies in which the mission is interested (range $[10^{-6}, 10^{-1}]$ kton TNT at the Earth). In particular, the more energetic impacts saturate the detectors of the two channels frequently. On the other hand, results suggest that the less energetic impacts are properly detected. Notably, more than the 99% of the detected impacts are resolved without saturating the detectors. That because of how meteoroids are distributed with respect to their impact kinetic energy. Performance is not degraded with the equipped 150 mm long baffle when straylight noise is taken into account.

5 Payload data return estimation

An estimation of the scientific data budget of the LUMIO mission has been performed to infer the data requirements. The estimation of the scientific data budget has been assessed exploiting MeGun and assuming the following scientific products to be downloaded:

- picture tiles of 50×50 pixels (frames cropped around the flash);
- 5 tiles saved per impact;
- 2 channels working synchronously (tiles from both channels downloaded);
- 2 bytes (16 bits) per pixel.

Moreover, since not all the meteoroids generated by MeGun can be observed by LUMIO, only the potentially detected impacts are retained. The events not retained are those that: *i*) impact the Moon in the illuminated side; *ii*) impact the Moon in the nearside; *iii*) impact the Moon when the illumination of the farside is greater than 50% [13]; *iv*) are out of the impact kinetic energy range $[10^{-6}, 10^{-1}]$ kton TNT at the Earth; *v*) whose visibility is obstructed by natural features (e.g., mountains) of the Moon (20% chance that this occurs).

The Monte Carlo analysis carried out is focused on the year 2024. The results are shown in Fig. 9. The statistical results have been obtained running 1000 scenarios. The plot shows clearly when LUMIO cannot perform the observation due to the unfavorable illumination conditions of the Moon. Indeed, there are windows approximately long 15 days that repeat periodically in which no scientific data are produced. These periods shift in time from year to year. Note that during the year 2024, the daily data rate in correspondence of the Geminids shower is particularly high, reaching a peak greater than 100 Mbit deg^{-1}. That because, in year 2024, the favorable illumination condition allows to observe the peak of the Geminids meteoroid shower. For what concerns the overall scientific data budget, almost 5 Gbit of data are expected to be produced for an operative phase lasting 1 year.

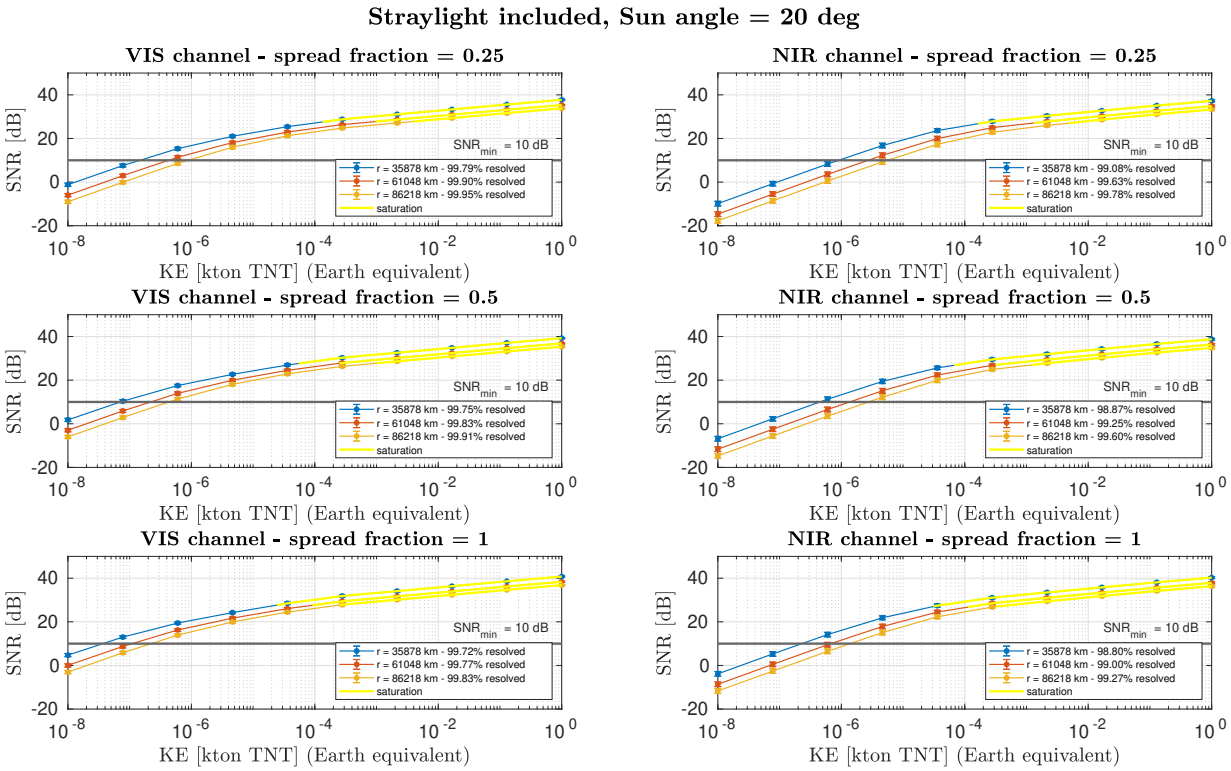

Fig. 8: Radiometric analysis about impact flash detection accounting for straylight, Sun angle equal to 20 deg. The SNR as a function of the impact kinetic energy in Earth equivalent is drawn for significant cases. The plots show how the SNR varies in the two channels for the 3 different cases of flash impact peak location within the central pixel of the detector. In each chart the SNR for different distances from the Moon of LUMIO is plotted. In yellow are identified the impact kinetic energies that saturate the detectors. The black horizontal line marks the conservative threshold of minimum SNR. The legends contain information about the percentage of detected impacts which do not saturate the LUMIO-Cam. Gain G fixed at 10. For each given impact kinetic energy, 1000 impacts have been simulated. Semi-log scale plots.

6 Conclusions

LUMIO lunar CubeSat is one of the two winner of ESA's LUCE SysNova competition. The phase A study has been conducted during 2020 and successfully completed at the beginning of 2021 under ESA's GSTP contract, after an independent mission assessment performed by ESA's CDF team.

LUMIO is a 12U XL CubeSat equipped with the LUMIO-Cam, an optical instrument capable of detecting impact flashes to continuously monitor and process the data. The mission implements a sophisticated transfer phase and orbit design, and will make use of the most advanced COTS CubeSat technology to serve as a demonstrator for the use of CubeSats as viable, low-cost platform for interplanetary science and exploration missions.

In this work, an overview of the mission, the concept of operations, and a prediction of the payload data return of the LUMIO lunar CubeSat have been presented. The modeling of the LUMIO-Cam has been discussed in detail. Results coming from the performed radiometric analysis accounting for straylight noise have been presented. According to the radiometric analysis results, the design of the LUMIO-Cam satisfies the payload functional requirements of the LUMIO mission.

Acknowledgments

Part of this work has been conducted under ESA Contract No. 4000130257/20/NL/AS under the GSTP and has received support from the national delegations of Italy (ASI), the Netherlands (NSO) and Norway (NOSA).

Bibliography

[1] Z Ceplecha, J Borovička, W G Elford, D O ReVelle, R L Hawkes, V Porubčan, and M Šimek.

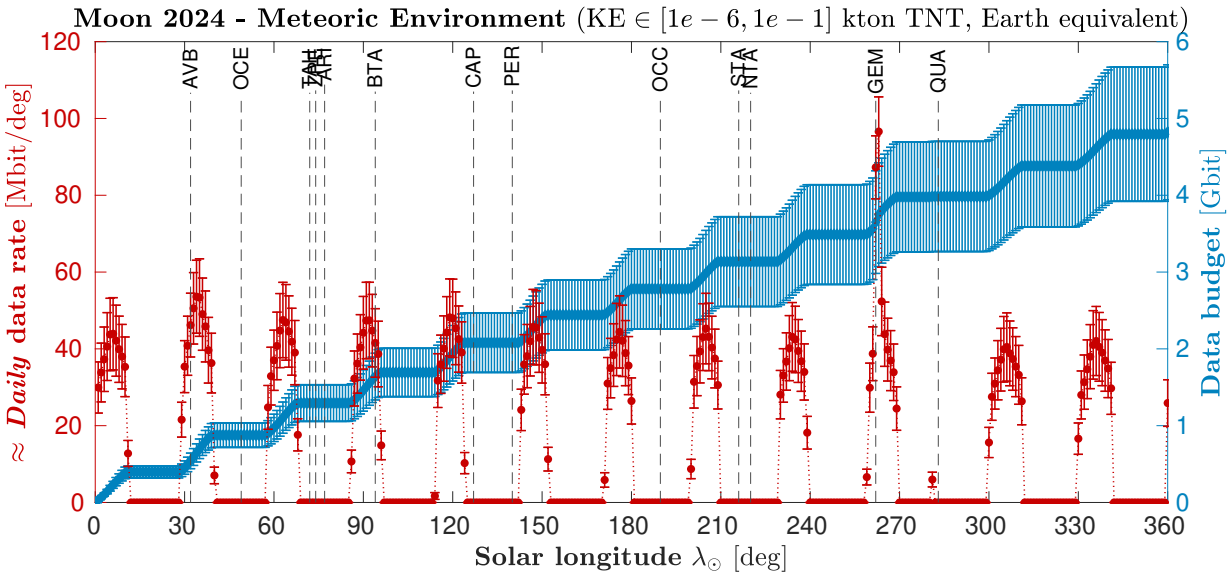

Fig. 9: Payload data return estimation – year 2024. On the y-left axis, in red, daily data rate as a function of solar longitude. On the y-right axis, in blue, cumulative data budget as a function of solar longitude. 1 year time window, from 01/01/2024 to 01/01/2025. Results shown in 1 deg bins. Stray light noise neglected. Statistical results obtained from 1000 runs.

Meteor phenomena and bodies. *Space Science Reviews*, 84(3-4):327–471, 1998. DOI: 10.1023/A:1005069928850.

[2] J Oberst, A Christou, R Suggs, D Moser, I J Daubar, A S McEwen, M Burchell, T Kawamura, H Hiesinger, K Wünnemann, et al. The present-day flux of large meteoroids on the lunar surface—a synthesis of models and observational techniques. *Planetary and Space Science*, 74(1):179–193, 2012. DOI: 10.1016/j.pss.2012.10.005.

[3] L R Bellot Rubio, J L Ortiz, and P V Sada. Luminous efficiency in hypervelocity impacts from the 1999 lunar leonids. *The Astrophysical Journal Letters*, 542(1):L65–L68, 2000. DOI: 10.1086/312914.

[4] Detlef Koschny and Jonathan McAuliffe. Estimating the number of impact flashes visible on the Moon from an orbiting camera. *Meteoritics and Planetary Science*, 44(12):1871–1875, 2009. DOI: 10.1111/j.1945-5100.2009.tb01996.x.

[5] J L Ortiz, J M Madiedo, N Morales, P Santos-Sanz, and F J Aceituno. Lunar impact flashes from geminids: analysis of luminous efficiencies and the flux of large meteoroids on earth. *Monthly Notices of the Royal Astronomical Society*, 454(1):344–352, 2015. DOI: 10.1093/mnras/stv1921.

[6] R M Suggs, D E Moser, W J Cooke, and R J Suggs. The flux of kilogram-sized meteoroids from lunar impact monitoring. *Icarus*, 238:23–36, 2014. DOI: 10.1016/j.icarus.2014.04.032.

[7] A M Cipriano, D A Dei Tos, and F Topputo. Orbit design for lumio: The lunar meteoroid impacts observer. *Frontiers in Astronomy and Space Sciences*, 5:29, 2018. DOI: 10.3389/fspas.2018.00029.

[8] V Franzese, P Di Lizia, and F Topputo. Autonomous optical navigation for the lunar meteoroid impacts observer. *Journal of Guidance, Control, and Dynamics*, 42(7):1579–1586, 2019. DOI: 10.2514/1.g003999.

[9] R Walker, A Cropp, P Fernandez, M Simmonds, Q Mannes, P Concari, M Braghin, Y le Deuff, D de Wilde, A Herbertz, J van den Eynde, G Cifani, D Wegner, T Szewxzyk, J Vennekens, A Cipriano, A Piris Nino, M Branco, P Hager, L Desjonqueres, W Martens, A Kleinschneider, and L Bucci. Lumio cdf study final report, ref. cdf-r-36, february 2018, 2018.

[10] Herbert Raab. Detecting and measuring faint point sources with a CCD. In *Proceedings of Meeting on Asteroids and Comets in Europe (MACE)*, 2002.

[11] S Bouley, D Baratoux, J Vaubaillon, A Mocquet, M Le Feuvre, F Colas, Z Benkhaldoun, A Daassou, M Sabil, and Lognonné P. Power and duration of impact flashes on the moon: Implication for the

cause of radiation. *Icarus*, 218(1):115–124, 2012. DOI: 10.1016/j.icarus.2011.11.028.

[12] G Merisio, M Massari, P Di Lizia, J Biggs, C Giordano, V Franzese, F Topputo, D Koschny, J Vennekens, and R Walker. Predicting the outcome of the lumio lunar cubesat. In *71st International Astronautical Congress (IAC 2020)*, pages 1–14, 2020.

[13] J L Ortiz, F J Aceituno, J A Quesada, J Aceituno, M Fernández, P Santos-Sanz, J M Trigo-Rodríguez, J Llorca, F J Martín-Torres, P Montañés-Rodríguez, and E Pallé. Detection of sporadic impact flashes on the Moon: Implications for the luminous efficiency of hypervelocity impacts and derived terrestrial impact rates. *Icarus*, 184(2):319–326, 2006. DOI: 10.1016/j.icarus.2006.05.002.